

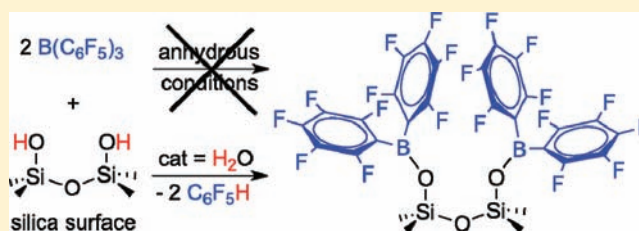
Borane-Induced Dehydration of Silica and the Ensuing Water-Catalyzed Grafting of $B(C_6F_5)_3$ To Give a Supported, Single-Site Lewis Acid, $\equiv SiOB(C_6F_5)_2$

Ying-Jen Wanglee,[†] Jerry Hu,[‡] Rosemary E. White,[§] Ming-Yung Lee,[§] S. Michael Stewart,[§] Philippe Perrotin,[§] and Susannah L. Scott^{*,†,§}

[†]Department of Chemistry & Biochemistry, [‡]Materials Research Laboratory, and [§]Department of Chemical Engineering, University of California, Santa Barbara, California 93106, United States

Supporting Information

ABSTRACT: A supported, single-site Lewis acid, $\equiv SiOB(C_6F_5)_2$, was prepared by water-catalyzed grafting of $B(C_6F_5)_3$ onto the surface of amorphous silica, and its subsequent use as a cocatalyst for heterogeneous olefin polymerization was explored. Although $B(C_6F_5)_3$ has been reported to be unreactive toward silica in the absence of a Brønsted base, we find that it can be grafted even at room temperature, albeit slowly. The mechanism was investigated by 1H and ^{19}F NMR, in both the solution and solid states. In the presence of a trace amount of H_2O , either added intentionally or formed *in situ* by borane-induced dehydration of silanol pairs, the adduct $(C_6F_5)_3B \cdot OH_2$ hydrolyzes to afford C_6F_5H and $(C_6F_5)_2BOH$. The latter reacts with the surface hydroxyl groups of silica to yield $\equiv SiOB(C_6F_5)_2$ sites and regenerate H_2O . When $B(C_6F_5)_3$ is present in excess, the resulting grafted boranes appear to be completely dry, due to the eventual formation of $[(C_6F_5)_2B]_2O$. The immobilized, tri-coordinate Lewis acid sites were characterized by solid-state ^{11}B and ^{19}F NMR, IR, elemental analysis, and C_3H_5N -TPD. Their ability to activate two molecular C_2H_4 polymerization catalysts, Cp_2ZrMe_2 and an (α -iminocarboxamidato)nickel(II) complex, was explored.



INTRODUCTION

Strong Lewis acids such as alkylaluminums and alkylaluminumoxanes, as well as various mono- and dinuclear boranes, are used commercially as cocatalysts in the coordination polymerization of α -olefins.¹ $B(C_6F_5)_3$ has emerged as a preferred cocatalyst in solution-state metallocene-mediated olefin polymerization, because it is well-defined, non-pyrophoric, and effective in a stoichiometric amount. The highly acidic borane extracts an alkyl ligand from a dialkylmetallocene, giving a bulky, weakly coordinating counteranion, $RB(C_6F_5)_3^-$. It stabilizes the alkylmetallocenium cation,² but is readily displaced from the coordination sphere of the transition metal to allow the olefin substrate to bind. In an interesting variation, $B(C_6F_5)_3$ activates (α -iminocarboxamidato)nickel(II) catalyst precursors remotely by binding to a carbonyl group in the ligand backbone, forming zwitterionic active sites to which coordination of the olefin and the borate co-catalyst do not compete.³

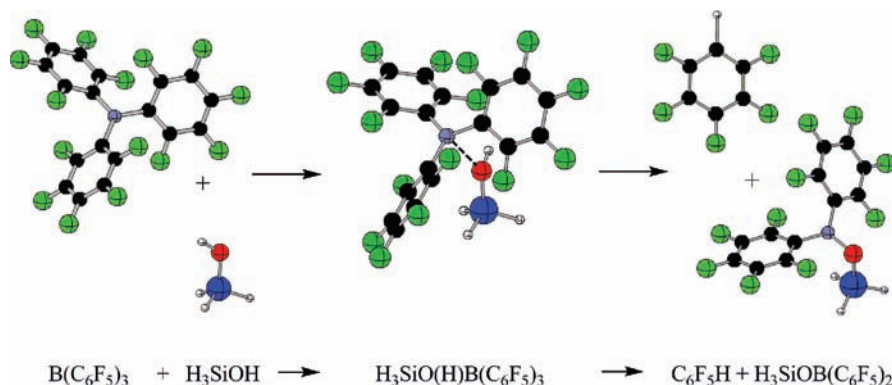
Heterogeneous Lewis acids are important in many catalytic processes, including the Friedel–Crafts⁴ and Diels–Alder reactions,⁵ in addition to α -olefin polymerization.^{1,6} Supported polymerization catalysts have several well-known advantages relative to their homogeneous analogues, including lower operating temperatures in continuous gas-phase or slurry reactors, reduced reactor fouling, and better control of polymer particle morphology.^{6,7} Silica is the most common support for single-site polymerization catalysts, because of its favorable fragmentation

properties during the reaction. Its surface hydroxyl content can be controlled simply by thermal treatment.⁸ An effective catalyst immobilization strategy involves anchoring the Lewis acidic cocatalyst onto the support via its reaction with these surface hydroxyl groups.⁶ For example, the widely used cocatalyst methylaluminumoxane reacts readily with silica. However, being a complex mixture of oligomers of varying Lewis acidity,⁹ it does not result in a well-defined supported Lewis acid. The consequent active-site heterogeneity when the catalyst is added is one of the factors responsible for the observed broadening of the molecular weight distribution when single-site olefin polymerization catalysts are supported. Recently, there has been strong interest in creating more uniform supported cocatalysts for commercial ethylene polymerization processes.¹⁰

Silica directly modified with $B(C_6F_5)_3$ has been claimed to be effective as a supported cocatalyst for olefin polymerization,^{10a,11} although the material was not characterized, and the nature of the interaction was not specified. More detailed studies found that $B(C_6F_5)_3$ binds weakly to silica via adduct formation with surface hydroxyl groups,¹² or that $B(C_6F_5)_3$ is only physisorbed on silica.¹³ Hydrogen-bonding was shown to be responsible for the immobilization of tetrafluoroborate salts of Pd and Ru complexes onto silica.¹⁴

Received: August 18, 2011

Published: November 22, 2011

Scheme 1. Calculated Structures Used To Explore the Protonolysis of $B(C_6F_5)_3$ by H_3SiOH^a 

^aColor scheme: B, gray; C, black; F, green; Si, blue; O, red; H, white. Overall $\Delta E = -111.7$ kJ/mol.

In contrast to this apparent lack of success in direct grafting by $B(C_6F_5)_3$, its immobilization onto silica was achieved in the presence of R_2NPh ($R = Me$ and Et) or $n-BuLi/Ph_3CCl$, via the formation of ion-pairs such as $[HNR_2Ph^+][(\equiv SiO)B(C_6F_5)_3^-]$ or $[Ph_3C^+][(\equiv SiO)B(C_6F_5)_3^-]$.^{10a,15} The former was reported to activate Cp^*ZrMe_3 for ethylene polymerization.^{13,16} However, a detailed study involving a molecular silsesquioxane analogue found that ion-pair formation is readily reversible, and free $B(C_6F_5)_3$ is released into solution.¹⁷ The subsequent polymerization activity likely does not involve a supported catalyst.

In the present work, we investigate the direct reaction of $B(C_6F_5)_3$ with silica. Unlike previous reports,^{12,13} we find that irreversible, covalent grafting of the borane does occur, but only when a trace of H_2O is present. We also demonstrate the effectiveness of the resulting $\equiv SiOB(C_6F_5)_2$ sites as cocatalysts in the activation of an (α -iminocarboxamidato)nickel(II) complex. In this family of late transition metal catalysts, the substituents on the aryl groups of the supporting ligand modulate reactivity and thereby influence the microstructure of the polyolefin produced.^{3,18} Since related late transition metal catalysts can copolymerize ethylene with polar comonomers,¹⁹ the possibility exists to use supported versions of these catalysts to create new classes of polymeric materials with interesting properties.

RESULTS

Computational Study of the Possible Reactions between $B(C_6F_5)_3$ and H_3SiOH . Previous investigators failed to observe a reaction between $B(C_6F_5)_3$ and the hydroxyl-terminated surfaces of amorphous silica experimentally.^{12,13} The feasibility of direct protonolysis of $B(C_6F_5)_3$ by a simple silanol, H_3SiOH , was investigated computationally. The calculated minimum energy structure of $B(C_6F_5)_3$ is trigonal planar at B, with C–B–C angles of 120° and B–C bond lengths of 1.57 Å, consistent with previous results.²⁰ Initial formation of the silanol adduct results in a slight decrease in the C–B–C angles to 113 – 117° (Scheme 1), but the B–O distance remains extremely long, at 1.69 Å. The expected reaction product, $H_3SiOB(C_6F_5)_2$, has a much shorter B–O bond, 1.34 Å, as well as trigonal geometry, with C–B–C and C–B–O angles of 122 and 121° , respectively. Liberation of C_6F_5H is exothermic, $\Delta E = -111.7$ kJ/mol, relative to the separated reactants.

These calculations suggest that direct protonolysis of $B(C_6F_5)_3$ by silica is thermodynamically favorable, although it may be prohibitively slow. In the calculated IR spectrum of

$B(C_6F_5)_3$, the most intense band occurs at 1441 cm^{-1} . It represents modes that involve B–C stretching, B–C scissoring, and ring breathing. In $H_3SiOB(C_6F_5)_2$, it undergoes a slight blue-shift to 1446 cm^{-1} and gains intensity, as it acquires a major contribution from B–O stretching. This predicted change in the IR spectrum is expected to be diagnostic of covalent bonding between boron and silica (see below).

Reaction of $B(C_6F_5)_3$ with A380-200 Silica. The silica was first pretreated at 200 °C under vacuum (A380-200) to remove adsorbed H_2O without inducing dehydroxylation of the silica surface. This solid was mixed with solid $B(C_6F_5)_3$ (0.56 wt % B, B/accessible $\equiv SiOH = 0.42$), and the evolution of the mixture was studied by solid-state 1H MAS NMR. The spectrum of unmodified A380-200 consists of two broad, overlapping signals (Figure 1a). The relatively narrow peak at

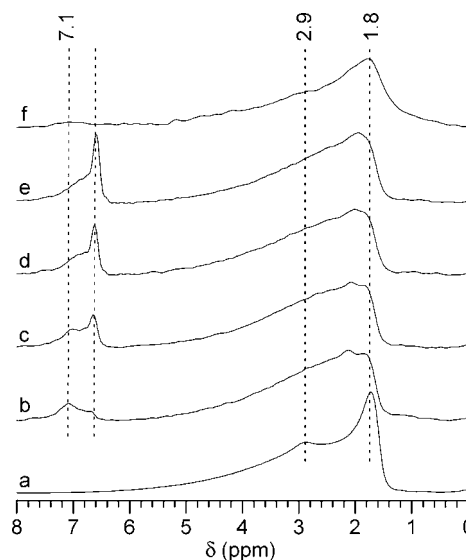


Figure 1. Solid-state 1H MAS NMR spectra of A380-200, (a) before and (b–e) at various times during its room-temperature reaction with solid $B(C_6F_5)_3$ ($B/\equiv SiOH = 0.42$): (b) after 3 h, (c) after 7 h, (d) after 1 d, (e) after 3 d, (f) after washing the previous sample with toluene- d_8 . Recorded with 14 kHz MAS.

1.8 ppm is assigned to the protons of non-hydrogen-bonded surface hydroxyl groups, while the broad peak centered at 2.9 ppm corresponds to hydroxyl protons deshielded by a range of hydrogen-bonding interactions.²¹ In the presence of $B(C_6F_5)_3$,

the intensity of the latter signal increased relative to that of the former (Figure 1b), indicating that some of the non-hydrogen-bonded surface hydroxyls of the silica are perturbed by hydrogen-bonding to $B(C_6F_5)_3$ (eq 1). In addition, two new



signals appeared, at 6.8 and 7.1 ppm. The former gained intensity over the course of 3 d at room temperature, while the latter became relatively less intense (Figure 1b–e). The signal at 7.1 ppm therefore corresponds to an intermediate that is eventually consumed during the reaction, while the signal at 6.8 ppm corresponds to a reaction product. Upon washing the solid mixture with dry toluene- d_8 , both signals at 6.8 and 7.1 ppm disappeared (Figure 1f). This further identifies them as weakly adsorbed species that are not covalently bonded to the silica surface. The signal at 6.8 ppm was assigned to the expected grafting product C_6F_5H , based on the solid-state 1H MAS NMR spectrum of an authentic C_6F_5H /silica mixture (Figure S1). It is shifted downfield from its solution-state value (C_7D_8 , δ 5.80 ppm) by interaction with the silica, presumably H-bonding involving the surface silanols.

The evolution of the solid-state ^{19}F MAS NMR spectrum of the $B(C_6F_5)_3$ /A380-200 mixture is shown in Figure 2. Three

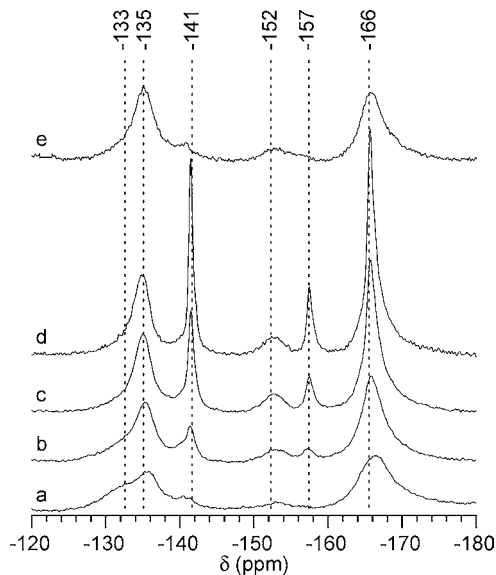


Figure 2. Solid-state ^{19}F MAS NMR spectra (282 MHz) recorded during the room-temperature reaction of $B(C_6F_5)_3$ with A380-200 ($B/\equiv SiOH = 0.42$): (a) after 3 h, (b) after 7 h, (c) after 1 d, (d) after 3 d, and (e) after washing the sample with toluene- d_8 . Recorded with 14 kHz MAS.

chemical shift regions are characteristic of the C_6F_5 ring: *o*-F ($-125 < \delta < -140$ ppm), *p*-F ($-140 < \delta < -155$ ppm), and *m*-F ($-155 < \delta < -165$ ppm). Initially, all of the signals are very broad, with maxima at -136 , -153 , and -166 ppm (Figure 2a). Nevertheless, in the *o*-F region, two clear shoulders are visible on the signal at -135 ppm, at -133 and -141 ppm, implying that there are at least three distinct types of C_6F_5 rings present. Over several hours, the shoulder at -133 ppm (assigned to $B(C_6F_5)_3$ interacting with the surface hydroxyls of silica) disappeared, while the shoulder at -141 ppm grew in intensity and became sharper. In the *p*-F region, a signal appeared at

-157 ppm and gradually became sharper, while the signal at -166 ppm in the *m*-F region shifted very slightly and narrowed appreciably. After 3 d, three narrow signals were apparent, at -141 , -157 , and -166 ppm. They are attributed to C_6F_5H , on the basis of the solid-state ^{19}F MAS NMR spectrum of an authentic C_6F_5H /silica mixture (Figure S2). The three broad signals (-135 , -152 , and -166 ppm) remaining in the solid-state ^{19}F MAS NMR spectrum of the washed solid (Figure 2e) are assigned to grafted boranes, $(\equiv SiO)_nB(C_6F_5)_{3-n}$ produced according to eq 2. Further evidence for the formulation of the grafted species is presented below.



The mechanism of the slow grafting reaction was further investigated by analyzing extractable reaction intermediates. In the solution-state 1H NMR spectrum of the toluene- d_8 washing solution, three signals at 4.75, 5.80, and 6.28 ppm are visible (Figure 3a). They are assigned to $(C_6F_5)_3B \cdot OH_2$, C_6F_5H , and

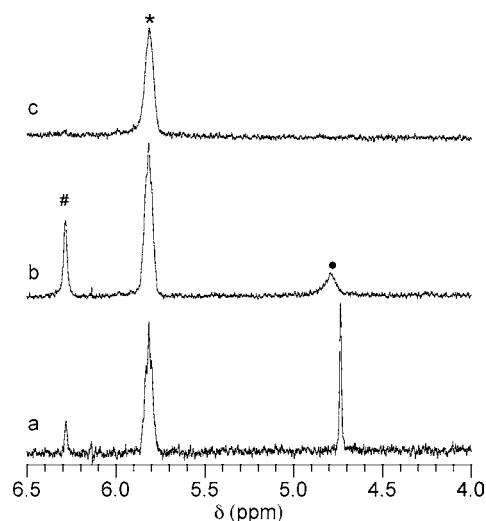
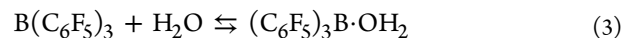


Figure 3. Solution-state 1H NMR spectra of toluene- d_8 used to wash a solid mixture of $B(C_6F_5)_3$ and A380-200 ($B/\equiv SiOH = 0.42$): (a) after 3 d, (b) after 33 d, and (c) after 80 d. Signals are marked for C_6F_5H (*), $(C_6F_5)_2B(OH)$ (#), and $B(C_6F_5)_3/H_2O$ mixture (●).

$(C_6F_5)_2BOH$, respectively, by comparison to authentic samples.^{12,22} The peak at 5.80 ppm is broader than the others, due to 1H - ^{19}F *J*-coupling.²³ The appearance of $(C_6F_5)_3B \cdot OH_2$ requires the presence of H_2O (eq 3), although no free H_2O was



observed by solution-state 1H NMR (0.33 ppm). The equilibrium shown in eq 3 will be displaced to the right when the amount of water is much less than that of $B(C_6F_5)_3$.

The solution-state ^{19}F NMR spectrum of the toluene wash obtained after 3 d reaction (Figure 4a) is consistent with these assignments. The set of broad signals at -128.4 , -141.5 , and -159.6 ppm is assigned to $B(C_6F_5)_3$ in dynamic exchange with $(C_6F_5)_3B \cdot OH_2$. On the basis of their chemical shifts, the set of narrow, weak signals at -132.4 , -147.5 , and -160.6 ppm is assigned to $(C_6F_5)_2BOH$.¹² A third set of narrow signals at -138.5 , -153.5 , and -161.8 ppm is characteristic of C_6F_5H .¹²

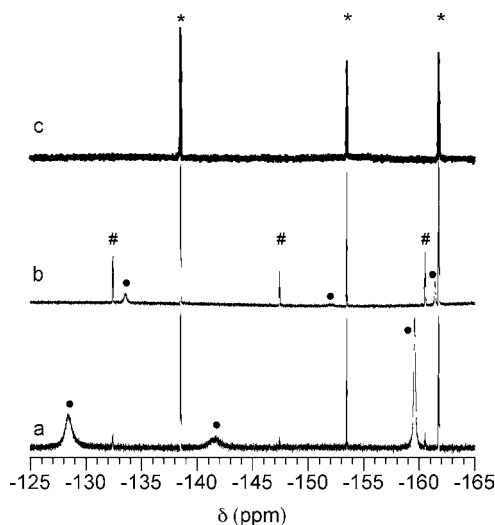


Figure 4. Solution-state ^{19}F NMR spectra of toluene- d_8 used to wash a solid mixture of $\text{B}(\text{C}_6\text{F}_5)_3$ and A380-200 ($\text{B}/\equiv\text{SiOH} = 0.42$): (a) after 3 d, (b) after 33 d, and (c) after 80 d. Signals are marked for $\text{C}_6\text{F}_5\text{H}$ (*), $(\text{C}_6\text{F}_5)_2\text{B}(\text{OH})$ (#), and $\text{B}(\text{C}_6\text{F}_5)_3/\text{H}_2\text{O}$ mixture (•).

Peak positions and assignments for all toluene-extractable species are summarized in Table S1.

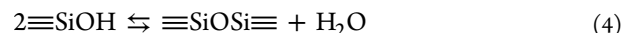
Since the solid–solid reaction was clearly incomplete even after 3 d at room temperature, the reaction progress was monitored at longer times, by washing portions of the solid with dry toluene- d_8 and analyzing the solutions with ^1H and ^{19}F NMR. After 33 d, the ^1H signals at 5.80 and 6.28 ppm were still present; however, the sharp signal at 4.75 ppm had shifted to 4.80 ppm and broadened (Figure 3b). The increased line width indicates that the $\text{B}(\text{C}_6\text{F}_5)_3/\text{H}_2\text{O}$ ratio (i.e., the $(\text{C}_6\text{F}_5)_3\text{B}/(\text{C}_6\text{F}_5)_3\text{B}\cdot\text{OH}_2$ ratio) decreases over time.²² After 33 d, the solution-state ^{19}F NMR spectrum still showed three sets of three signals (Figure 4b). The narrow signals attributed to $(\text{C}_6\text{F}_5)_2\text{BOH}$ and $\text{C}_6\text{F}_5\text{H}$ remained, but the broad signals of $\text{B}(\text{C}_6\text{F}_5)_3$ in dynamic exchange with $\text{B}(\text{C}_6\text{F}_5)_3\cdot\text{OH}_2$ had weakened and shifted significantly, appearing at -133.6 , -152.0 , and -161.4 ppm. These peak positions indicate that the $\text{B}(\text{C}_6\text{F}_5)_3/\text{H}_2\text{O}$ ratio was ca. 1.25.²²

After 80 d, the solution-state ^1H NMR spectrum consisted of only one signal for $\text{C}_6\text{F}_5\text{H}$, at 5.80 ppm (Figure 3c). The intermediates $(\text{C}_6\text{F}_5)_3\text{B}\cdot\text{OH}_2$ and $(\text{C}_6\text{F}_5)_2\text{BOH}$ are therefore consumed as the reaction between $\text{B}(\text{C}_6\text{F}_5)_3$ and A380-200 proceeds. Free H_2O was not extracted by toluene and may be coordinated to the grafted borane or hydrogen-bonded to the surface hydroxyls of silica. In the solution-state ^{19}F NMR

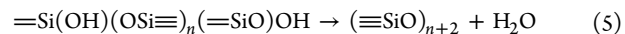
spectrum, the only signals remaining were those for $\text{C}_6\text{F}_5\text{H}$ (Figure 4c). The boron content of the solid product, 0.58 wt %, was essentially the same as the initial value, 0.56 wt %.

The reaction between $\text{B}(\text{C}_6\text{F}_5)_3$ and A380-200 ($\text{B}/\equiv\text{SiOH} = 0.41$) is much faster when conducted in an air-free solution-state NMR tube in the presence of toluene- d_8 at 100 °C. Similar to the results described above, $(\text{C}_6\text{F}_5)_3\text{B}\cdot\text{OH}_2$ and $(\text{C}_6\text{F}_5)_2\text{BOH}$ were observed in solution as intermediates, as well as $[(\text{C}_6\text{F}_5)_2\text{B}]_2\text{O}$ (from the reversible, temperature-dependent condensation of $(\text{C}_6\text{F}_5)_2\text{BOH}$). $\text{C}_6\text{F}_5\text{H}$ was the only soluble product present after 3 d (see Figures S3 and S4). The C/B ratio of the recovered solid was 9.0 ± 0.1 , suggesting the presence of a mixture of $\equiv\text{SiOB}(\text{C}_6\text{F}_5)_2$ and $(\equiv\text{SiO})_2\text{BC}_6\text{F}_5$ sites.

Computational Study of $\text{B}(\text{C}_6\text{F}_5)_3$ -Induced Silica Dehydration. Since the A380-200 silica used in the reaction with $\text{B}(\text{C}_6\text{F}_5)_3$ was initially completely free of molecular water (see Experimental Section), we suspected that the H_2O observed coordinated to $\text{B}(\text{C}_6\text{F}_5)_3$ arose by spontaneous condensation of silica hydroxyls (eq 4). Presumably, the presence of unreacted $\text{B}(\text{C}_6\text{F}_5)_3$ drives this reaction forward by binding H_2O (eq 3).



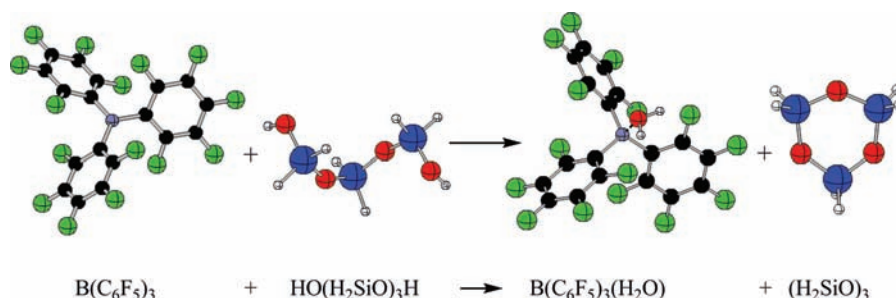
This $\text{B}(\text{C}_6\text{F}_5)_3$ -promoted dehydration of silica was explored computationally. When a pair of proximal hydroxyl groups condenses, a siloxane ring is formed (eq 5). Experimentally, the



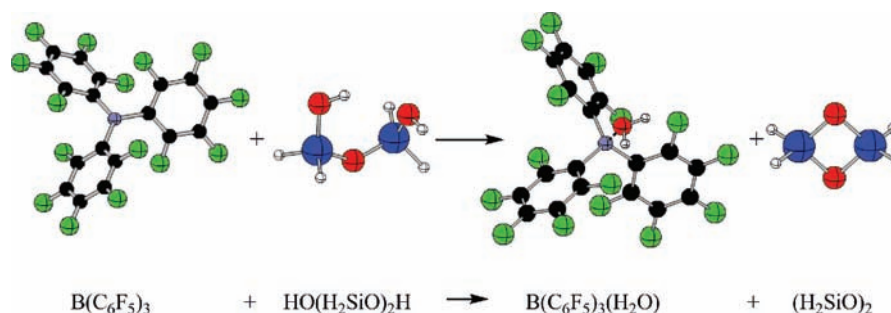
onset of this process is observed on fumed silicas above 200 °C,⁸ and the first-formed rings are relatively unstrained ($n \geq 2$). Raman signals characteristic of moderately strained trisiloxane rings ($n = 1$) reach their maximum intensity at ca. 500 °C, while IR signals for highly strained disiloxane rings ($n = 0$) are not observed until the temperature exceeds 600 °C.⁸ Since the hydroxyl groups of silica do not migrate at any of these temperatures,^{8,24} vicinal hydroxyl pairs (i.e., silanols separated by a single siloxane bond) that would form disiloxane rings if they condensed are necessarily still present on silicas pretreated at 500 °C.²⁵ Nonvicinal hydroxyl pairs (proximal, but separated by two or more siloxane bonds) occur on silicas pretreated at 200 °C⁸ but are largely eliminated by 500 °C. We note that only nonvicinal hydroxyl pairs (i.e., not vicinal hydroxyl pairs) can engage in mutual hydrogen-bonding.²⁶

Dehydration of a nonvicinal silanol pair to form a trisiloxane ring with moderate ring strain, representing dehydration of

Scheme 2. Dehydration of a Pair of Nonvicinal Silanols by $\text{B}(\text{C}_6\text{F}_5)_3$ ^a



^aColor scheme: B, gray; C, black; F, green; Si, blue; O, red; H, white. $\Delta E = -24.3$ kJ/mol.

Scheme 3. Dehydration of a Vicinal Silanol Pair by $B(C_6F_5)_3$ ^a

^aColor scheme: B, gray; C, black; F, green; Si, blue; O, red; H, white. $\Delta E = +84.5$ kJ/mol.

A380-200, is exothermic by -24.3 kJ/mol when the liberated water is coordinated to $B(C_6F_5)_3$ (Scheme 2). In contrast, borane-induced dehydration of a vicinal silanol pair to form a highly strained disiloxane ring, representing the dehydration of A380-500,⁸ is endothermic by 85.4 kJ/mol, even when the water is similarly captured (Scheme 3). Consequently, we expect $B(C_6F_5)_3$ to form $(C_6F_5)_3B \cdot OH_2$ when mixed with A380-200, but not with A380-500.

Reaction of $B(C_6F_5)_3$ with A380-500 Silica. In order to test the prediction that $B(C_6F_5)_3$ is unable to promote dehydration of vicinal silanol pairs, we attempted the reaction of $B(C_6F_5)_3$ with silica pretreated at 500 °C (A380-500). An NMR tube experiment was carried out, with the silica suspended in toluene- d_8 at 100 °C ($B/\equiv SiOH = 0.49$). After 24 h, the only soluble product observed in the solution-state NMR spectra was a trace of C_6F_5H (Figures S5 and S6). Significantly, no signals for H_2O , $(C_6F_5)_3B \cdot OH_2$, $(C_6F_5)_2BOH$, or $[(C_6F_5)_2B]_2O$ were detected. Dehydration is therefore much slower compared to the reaction on the more extensively hydroxylated silica (A380-200), and most $B(C_6F_5)_3$ remained unreacted.

These observations suggest that H_2O plays an essential role in the grafting of $B(C_6F_5)_3$, and that a well-defined, supported borane might be prepared on the more dehydroxylated silica using a catalytic amount of extrinsic H_2O . Therefore, we attempted the reaction of excess $B(C_6F_5)_3$ with A380-500 in toluene- d_8 ($B/\equiv SiOH = 4.6$) in the presence of added H_2O ($H_2O/\equiv SiOH = 0.1$). After heating the mixture at 100 °C for 3 d, the solid was washed with dry toluene and then dried in vacuum at 100 °C for 2.5 h. The solution-state ^{19}F NMR spectrum of the filtrate showed no evidence for H_2O , although $B(C_6F_5)_3$, $[(C_6F_5)_2B]_2O$, and C_6F_5H were all present (Figure S7). In the solid-state ^{19}F MAS NMR spectrum of the washed solid, the three signals of the grafted borane were observed at -135 , -152 , and -166 ppm (Figure 5). The solid-state ^{11}B MAS NMR spectrum contains a broad signal with a complex line shape (Figure S8), consistent with a low-symmetry boron environment.

The final B content of the solid, 0.72 wt %, corresponds to a loading of 0.87 mmol of B per gram of SiO_2 . Since the accessible hydroxyl content of the unmodified silica is 0.89 mmol of $\equiv SiOH/g$,²⁷ the reaction between $B(C_6F_5)_3$ and the surface hydroxyls is deemed to be essentially quantitative. Complete reaction of the accessible hydroxyls was confirmed by IR. The spectrum of unmodified A380-500 (Figure 6a) contains a narrow band at 3747 cm^{-1} assigned to non-hydrogen-bonded silanols and a weak, broad shoulder at 3670 cm^{-1} assigned to inaccessible silanols.⁸ The latter persist even when

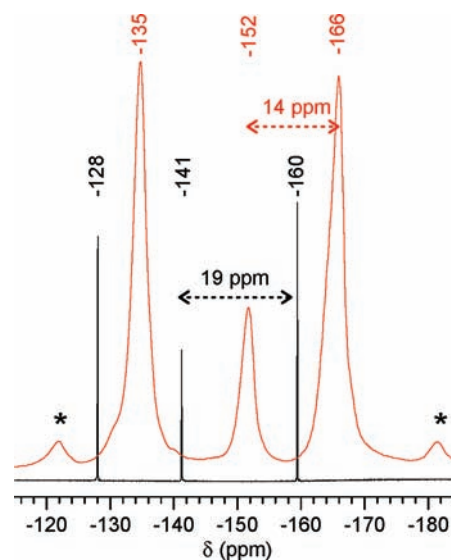


Figure 5. Comparison of the solid-state ^{19}F MAS NMR spectrum of A380-500, after its water-catalyzed reaction with $B(C_6F_5)_3$ (red), with the solution-state ^{19}F NMR spectrum 470 MHz of $B(C_6F_5)_3$ in toluene- d_8 (black). * designates a spinning sideband. Solid-state spectrum recorded with 14 kHz MAS.

silica is exposed to highly reactive metal complexes, such as $VOCl_3$ and $Ga(CH_3)_3$.^{25,27} After reaction with $B(C_6F_5)_3$ in the presence of a catalytic amount of H_2O , the peak at 3747 cm^{-1} disappeared, while the intensity of its shoulder did not change significantly (Figure 6b). This result demonstrates unequivocally that the surface hydroxyl groups are removed in the grafting reaction. Elemental analysis gave a final C/B ratio for the solid of 11.4 ± 1.4 , consistent with formulation of the product as $\equiv SiOB(C_6F_5)_2$.

Several vibrations are visible in the IR spectrum of $B(C_6F_5)_3$ in the range from 1650 to 1325 cm^{-1} (Figure 6c). The most intense, at 1472 cm^{-1} , represents modes that involve B–C stretching, C–B–C wagging, and ring-breathing, by comparison to the calculated spectrum (see above). It gains intensity and shifts to 1490 cm^{-1} in the spectrum of the borane-modified silica. This shift is consistent with a contribution from B–O stretching, and with the predicted change in the IR spectrum based on calculated spectra for $B(C_6F_5)_3$ and $H_3SiOB(C_6F_5)_2$ (see above). For comparison, the B–O stretching modes of silica-supported BF_3 and BCl_3 appear at 1452 and 1400 cm^{-1} , respectively.²⁸

Reaction of $(C_6F_5)_2BOH$ with A380-500 Silica. Since we detected $(C_6F_5)_2BOH$ in the reaction of $B(C_6F_5)_3$ with both

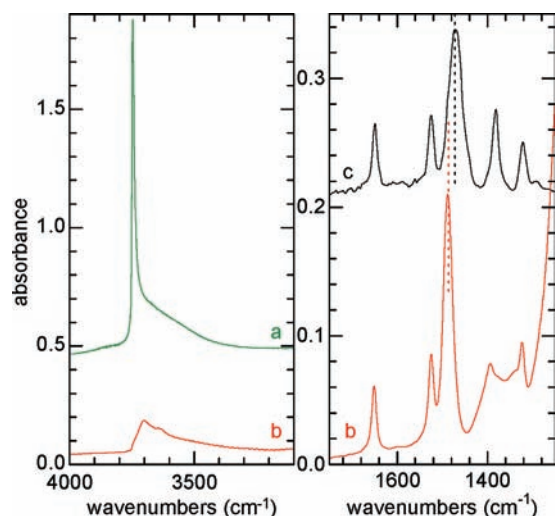
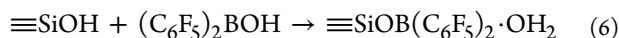


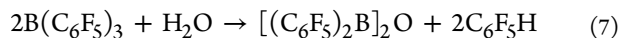
Figure 6. Transmission IR spectra of A380-500 silica: (a) before and (b) after modification with excess $B(C_6F_5)_3$ in the presence of 0.1 equiv of H_2O (relative to the accessible $\equiv SiOH$ content), followed by washing with toluene, compared with (c) neat $B(C_6F_5)_3$. Spectra are vertically offset for clarity.

types of silica and presumed it to be formed via the *in situ* hydrolysis of $(C_6F_5)_3B \cdot OH_2$, an authentic sample of the borinic acid was prepared¹² and its reactivity toward silica investigated. In the solution-state 1H and ^{19}F NMR spectra of a saturated toluene- d_8 solution prepared by mixing equal amounts of $B(C_6F_5)_3$ and H_2O , signals for both C_6F_5H and $(C_6F_5)_2BOH$ were observed, as reported previously.¹² In this solvent, soluble $(C_6F_5)_2BOH$ exists in equilibrium with insoluble $[(C_6F_5)_2BOH]_3$, observed as a white precipitate.

When this mixture was heated with A380-500 at 100 °C, the white precipitate of $[(C_6F_5)_2BOH]_3$ disappeared. After 2 h, only a trace of $(C_6F_5)_2BOH$ remained, according to the solution-state 1H and ^{19}F NMR spectra. Thus, $(C_6F_5)_2BOH$ does react readily with silica. The reaction generates H_2O as a stoichiometric product (eq 6). It presumably coordinates to the



grafted borane and quenches its Lewis acidity. A potential advantage of the H_2O -catalyzed grafting of $B(C_6F_5)_3$, as described above, is the much lower H_2O content of the product. Indeed, we believe the solid to be very dry when $B(C_6F_5)_3$ is initially present in excess, as a result of the eventual formation of $[(C_6F_5)_2B]_2O$ (eq 7).



Reaction of $B(C_6F_5)_3$ -Modified A380-500 Silica with C_5H_5N . In order to assess the number of types of Lewis acid sites present in the $B(C_6F_5)_3$ -modified silica, as well as their acid strength, the material was exposed to $C_5H_5N(g)$. In the solid-state ^{11}B MAS NMR spectrum, a single sharp, symmetrical peak was observed at -1.0 ppm (fwhm 5.5 ppm, 529 Hz) (Figure 7a). It contrasts with the broad, complex line shape observed for $\equiv SiOB(C_6F_5)_2$ (see above) and is consistent with conversion of the grafted B sites from trigonal to tetrahedral geometry. This change in local symmetry results in a significant reduction of the ^{11}B quadrupolar moment,²⁹

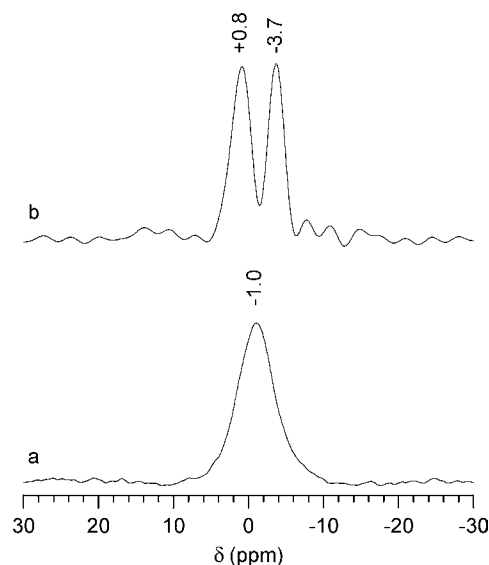
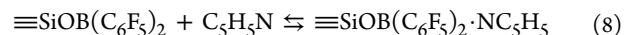


Figure 7. Solid-state ^{11}B MAS NMR spectra of $B(C_6F_5)_3$ -modified A380-500: (a) after C_5H_5N adsorption (96 MHz) and (b) after reaction with complex 1 (160 MHz). Both spectra were recorded using 14 kHz MAS.

with consequent NMR line narrowing. Temperature-programmed desorption of C_5H_5N from this material occurs at 200 °C as a single, symmetric peak (Figure S9). Thus we infer the presence of uniform Lewis acid sites, which react according to eq 8.



The IR spectrum of the borane-modified silica after pyridine adsorption is shown in Figure 8. The broad signal at 3670 cm^{-1} ,

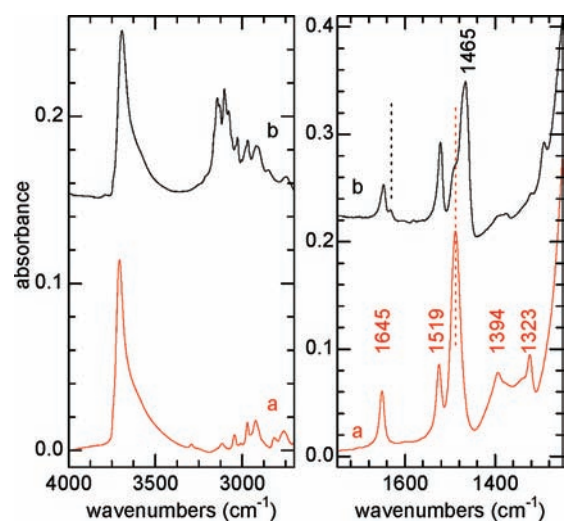


Figure 8. Transmission IR spectra of A380-500 silica: (a) after modification with $B(C_6F_5)_3$ and (b) followed by C_5H_5N adsorption.

assigned to inaccessible silanols, remains unchanged. The C–H stretches of adsorbed C_5H_5N are observed in the region 3200 – 3000 cm^{-1} . The positions of the C_6F_5 ring-breathing modes present at 1645 and 1519 cm^{-1} are essentially unaffected by the presence of pyridine. However, the band at 1490 cm^{-1} , which

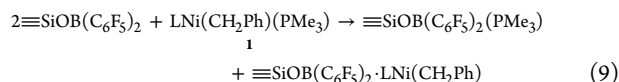
includes a contribution from B–O stretching, splits into two bands, at 1490 and 1465 cm^{-1} , upon coordination of B by N. New bands appear at 1632 and 1291 cm^{-1} . The former is characteristic of pyridine bound to a strong Lewis acid site.³⁰

Reaction of $\text{B}(\text{C}_6\text{F}_5)_3$ -Modified A380-500 Silica with $\text{Cp}_2\text{Zr}(\text{CH}_3)_2$. Despite the absence of accessible hydroxyl grafting sites, the reaction of $\text{Cp}_2\text{Zr}(\text{CH}_3)_2$ (0.19 mmol) with the borane-modified silica (200 mg, 0.13 mmol B) in toluene at room temperature for 4 h led to irreversible uptake about half of the metallocene: the recovered solid contained 2.5 wt % Zr, according to elemental analysis.

To create a supported catalyst, Cp_2ZrMe_2 (7.3 mg, 0.028 mmol) was sublimed for 2 d under reduced pressure (10^{-4} Torr) onto $\text{B}(\text{C}_6\text{F}_5)_3$ -modified A380-500 (30 mg, 0.020 mmol B) with the aid of a liquid N_2 bath. After reaction for 1 d at room temperature, and desorption of unreacted Cp_2ZrMe_2 at the same temperature for a further 2 d, C_2H_4 (111 Torr) was added at room temperature. The solid failed to initiate polymerization.

The fate of the metallocene was investigated using solution-state ^{19}F NMR. The reaction of $\text{Cp}_2\text{Zr}(\text{CH}_3)_2$ with $\equiv\text{SiOB}(\text{C}_6\text{F}_5)_2$ was performed in toluene- d_6 in an NMR tube ($\text{Zr}/\text{B} = 1.4$). After 40 min, two soluble products were observed by solution-state ^{19}F NMR (Figure S10). $(\text{CH}_3)_2\text{B}(\text{C}_6\text{F}_5)$ is responsible for three signals at -130.1 , -150.5 , and -161.9 ppm, while $\text{Cp}_2\text{Zr}(\text{CH}_3)(\text{C}_6\text{F}_5)$ gives rise to three signals at -114.4 , -155.8 , and -161.3 ppm (Table S2).^{17b,31} In addition, a set of minor signals at -132.0 , -165.1 , and -166.1 ppm may correspond to a tetra-coordinate borate, presumably the ion-pair $[\text{Cp}_2\text{ZrCH}_3^+][(\text{CH}_3)_2\text{B}(\text{C}_6\text{F}_5)_2^-]$.^{12,17b,31}

Reaction of $\text{B}(\text{C}_6\text{F}_5)_3$ -Modified A380-500 Silica with a Late Transition Metal Complex. We also explored the reaction of the borane-modified silica with $[N$ -(2,6-dimethylphenyl)-2-(2,6-dimethylphenylimino)propanamido- κ^2 - N,N](η^1 -benzyl)(trimethylphosphino)nickel(II) (**1**)^{18b} and the ability of this catalyst–co-catalyst combination to effect ethylene homopolymerization. The choice of **1** eliminates the ambiguity of heterogeneous vs homogeneous polymerization, since **1** is not a homogeneous catalyst for ethylene polymerization in the absence of a co-catalyst and produces only oligomers in the presence of soluble co-catalysts. Furthermore, no polymer is formed when a mixture of **1** and unmodified silica is exposed to ethylene. The expected reactions between the catalyst and the supported co-catalyst are shown in eq 9.



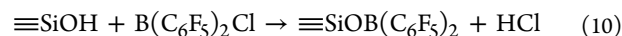
A mixture of **1** (3.5 mg, 0.0067 mmol Ni) and borane-modified silica (50 mg, 0.033 mmol B) was stirred in toluene (10 mL) for 3 h, and then toluene was removed under reduced pressure to yield an orange solid. As expected according to eq 9, the ^{11}B MAS NMR spectrum of the solid shows two narrow signals with comparable intensity at 0.8 ppm (fwhm 3.2 ppm, 513 Hz) and -3.7 ppm (fwhm 2.6 ppm, 417 Hz) (Figure 7b). Both peaks have chemical shifts and line widths characteristic of tetra-coordinate boron.³² In $\text{C}_6\text{D}_5\text{Br}$, $(\text{C}_6\text{F}_5)_3\text{B}\cdot\text{PMe}_3$ is reported to have a chemical shift of -14.7 ppm,³³ while a homogeneous analogue of the borane–**1** adduct has a chemical shift of -0.8 ppm in toluene.^{18a}

A slurry created by mixing a solution of **1** (0.22 mM) with the borane-modified silica (50 mg, $\text{B}/\text{Ni} = 4.7$) was fed ethylene on demand (5.2×10^3 Torr) for 30 min at 40 °C. The

amount of polyethylene (0.64 g) recovered from the reactor corresponds to a catalyst productivity of 190 g of PE (mmol Ni) $^{-1}$ h $^{-1}$. The polymer had a high molecular weight ($M_w = 185\,000$ g mol $^{-1}$, $M_w/M_n = 2.2$) and exhibited a single melt transition ($T_m = 125$ °C) by differential scanning calorimetry (DSC).

DISCUSSION

Reactivity of $\text{B}(\text{C}_6\text{F}_5)_3$ toward Silica. In previous studies, it was reported that $\text{B}(\text{C}_6\text{F}_5)_3$ does not react with silicas pretreated at 500, 700, or 1000 °C.^{12,13} The interaction of $\text{B}(\text{C}_6\text{F}_5)_3$ with a silsesquioxane monosilanol (modeling the hydroxyl-terminated surface of a partially dehydroxylated silica) yielded only a weakly bonded silanol adduct.¹³ In contrast, $\text{B}(\text{C}_6\text{F}_5)_2\text{Cl}$ reacts readily with both silica and soluble silsesquioxane trisilanols at room temperature.^{12,17b} A B–O bond is formed, and HCl is liberated (eq 10). Despite the similar Lewis acidities of $\text{B}(\text{C}_6\text{F}_5)_3$ and $\text{B}(\text{C}_6\text{F}_5)_2\text{Cl}$,²⁰ the steric bulk of the third pentafluorophenyl substituent apparently makes the direct reaction between $\text{B}(\text{C}_6\text{F}_5)_3$ and silanols (eq 2) very slow.

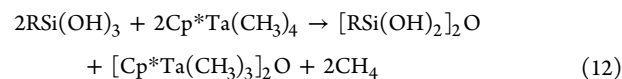


Mechanism of the Indirect Reaction between $\text{B}(\text{C}_6\text{F}_5)_3$ and Silica. Our results show that $\text{B}(\text{C}_6\text{F}_5)_3$ does react, albeit slowly, with dehydrated, but still highly hydroxylated, silica at ambient temperature. Over the course of 3 d, a mixture of $\text{B}(\text{C}_6\text{F}_5)_3$ and A380-200 generated $(\text{C}_6\text{F}_5)_3\text{B}\cdot\text{OH}_2$ and $\text{C}_6\text{F}_5\text{H}$. Since the reaction was conducted in the absence of adsorbed water, we infer that H_2O was formed by $\text{B}(\text{C}_6\text{F}_5)_3$ -promoted dehydration of the silica (eq 11). The dehydration reaction may



not involve the borane directly; it is possible that $\text{B}(\text{C}_6\text{F}_5)_3$ merely captures traces of H_2O generated by the unfavorable equilibrium in eq 4. In the case of A380-200, the new siloxane bond is likely associated with a trisiloxane (Si_3O_3) or larger ring.³⁴ Our DFT calculations show that formation of such rings is exothermic when accompanied by formation of $(\text{C}_6\text{F}_5)_3\text{B}\cdot\text{OH}_2$. The latter undergoes rapid exchange with free $\text{B}(\text{C}_6\text{F}_5)_3$, resulting in a characteristic broadening of the corresponding signals in the solution-state ^1H and ^{19}F NMR spectra^{15h,35} (Figures 3 and 4).

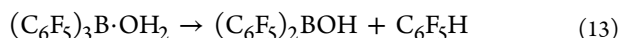
Chemical dehydration is a well-known reaction for molecular silanols. For example, although the silanetriol $(2,6\text{-}i\text{-Pr}_2\text{C}_6\text{H}_3)\text{-N}(\text{SiMe}_3)\text{Si}(\text{OH})_3$ is stable toward self-condensation, it underwent dehydration during its reaction with $\text{Cp}^*\text{Ta}(\text{CH}_3)_4$ (eq 12).³⁶ The resulting intermediates reacted further to yield



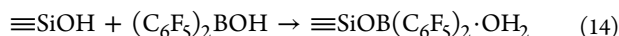
the isolated product, $[\text{Cp}^*\text{Ta}(\text{OH})(\text{O}_2\text{SiR})\text{O}]_2$. A similar mechanism was proposed for the reaction between $^t\text{BuSi}(\text{OH})_3$ and Re_2O_7 , leading to the perrhenate-substituted siloxane ring $[^t\text{BuSi}(\text{O})(\text{OREO}_3)]_4$.³⁷ The authors suggested that dehydration be considered in reactions of transition metal complexes with hydroxyl-terminated oxide surfaces, in addition to the frequently observed protonolysis of metal–ligand bonds. We believe that the reaction of $\text{B}(\text{C}_6\text{F}_5)_3$ with silica

described here is the first demonstration of this alternate grafting mechanism.

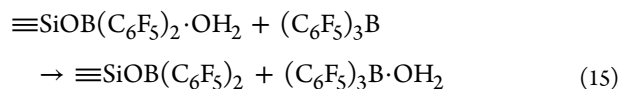
$(\text{C}_6\text{F}_5)_3\text{B}\cdot\text{OH}_2$ hydrolyzes slowly at room temperature to afford $(\text{C}_6\text{F}_5)_2\text{BOH}$ and $\text{C}_6\text{F}_5\text{H}$ (eq 13).^{12,20} This represents an



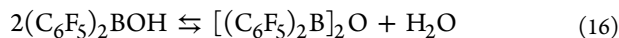
alternative to direct reaction with silanols (eq 2) for the formation of $\text{C}_6\text{F}_5\text{H}$. Although $(\text{C}_6\text{F}_5)_2\text{BOH}$ was indeed observed at room temperature and intermediate reaction times, it does not persist. It reacts with the surface hydroxyl groups (eq 14), as confirmed by the relatively rapid reaction of silica with an authentic sample of the borinic acid.



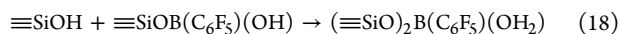
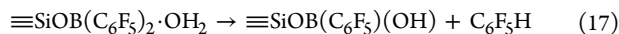
The net result is grafting of $\text{B}(\text{C}_6\text{F}_5)_3$ onto silica. Since H_2O is regenerated, its release from $\equiv\text{SiOB}(\text{C}_6\text{F}_5)_2\cdot\text{OH}_2$ and capture by free $\text{B}(\text{C}_6\text{F}_5)_3$ (eq 15) makes its role catalytic. All of the reactions involved in the water-catalyzed grafting of $\text{B}(\text{C}_6\text{F}_5)_3$ are summarized in Scheme 4.



At the higher reaction temperature (100 °C) with A380-200, $[(\text{C}_6\text{F}_5)_2\text{B}]_2\text{O}$ was also observed, while $(\text{C}_6\text{F}_5)_3\text{B}\cdot\text{OH}_2$ was not detected. At this temperature, hydrolysis of $(\text{C}_6\text{F}_5)_3\text{B}\cdot\text{OH}_2$ (eq 13) occurs rapidly. $[(\text{C}_6\text{F}_5)_2\text{B}]_2\text{O}$ arises by reversible condensation of $(\text{C}_6\text{F}_5)_2\text{BOH}$ (eq 16).²² After 3 d at 100 °C in the presence



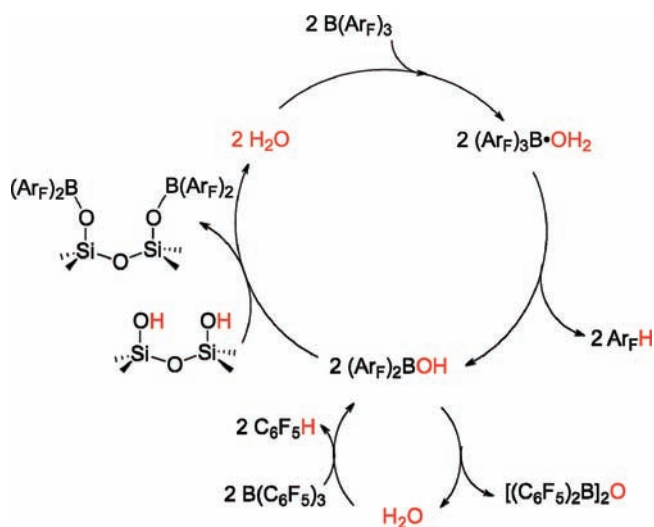
of A380-200 containing excess $\equiv\text{SiOH}$, both $[(\text{C}_6\text{F}_5)_2\text{B}]_2\text{O}$ and $\text{B}(\text{C}_6\text{F}_5)_2\text{OH}$ had disappeared, presumably via the irreversible reaction of $\text{B}(\text{C}_6\text{F}_5)_2\text{OH}$ with $\equiv\text{SiOH}$ (eq 14). The C/B ratio indicates that water transfer to unreacted $\text{B}(\text{C}_6\text{F}_5)_3$ (eq 15) competes with hydrolysis of $\equiv\text{SiOB}(\text{C}_6\text{F}_5)_2(\text{OH}_2)$ and further condensation with an adjacent silanol (eqs 17 and 18).



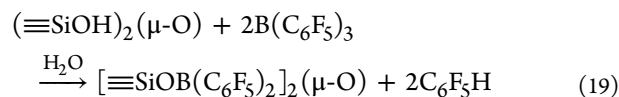
Thus, the reaction of $\text{B}(\text{C}_6\text{F}_5)_3$ with A380-200 occurs in several steps: silanol pair dehydration, hydrolysis of $(\text{C}_6\text{F}_5)_3\text{B}\cdot\text{OH}_2$, condensation of $(\text{C}_6\text{F}_5)_2\text{BOH}$ with a silanol, and (occasionally) further condensation of $\equiv\text{SiOB}(\text{C}_6\text{F}_5)_2$.

By comparison to its reaction with A380-200, the reaction of $\text{B}(\text{C}_6\text{F}_5)_3$ with A380-500 is very slow, and the expected products of silica dehydration, $(\text{C}_6\text{F}_5)_3\text{B}\cdot\text{OH}_2$ and $(\text{C}_6\text{F}_5)_2\text{BOH}$, were not observed. Nonvicinal silanol pairs that condense readily to form unstrained siloxane rings are no longer present once the silica has been heated to 500 °C,⁸ and our DFT calculations confirm that the $\text{B}(\text{C}_6\text{F}_5)_3$ -promoted dehydration of vicinal silanols to form highly strained 2-rings is endothermic. The inability to generate water via a reaction such as eq 11 precludes the subsequent water-catalyzed grafting reactions (eqs 13–15) on the more extensively dehydroxylated silica. Fortunately, grafting of $\text{B}(\text{C}_6\text{F}_5)_3$ onto A380-500 can be achieved by addition of a small amount of extrinsic H_2O (e.g.,

Scheme 4. Proposed Mechanism for Water-Catalyzed Grafting of $\text{B}(\text{C}_6\text{F}_5)_3$ onto Silica



10 mol %) as catalyst. The IR spectra in Figure 6 confirm that $\text{B}(\text{C}_6\text{F}_5)_3$ reacts essentially completely with the accessible surface hydroxyls. They are formulated as vicinal silanols in eq 19,



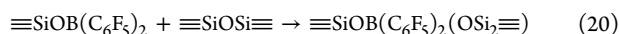
consistent with our recent studies of hydroxyl group disposition on this type of silica.^{25,38} The elemental analysis indicates that each vicinal pair reacts with two $\text{B}(\text{C}_6\text{F}_5)_3$, presumably to avoid the strain of a $[\text{Si}_2\text{BO}_3]$ ring. The solution-state ^{19}F NMR spectra in Figure S7 show that the added H_2O is eventually consumed by hydrolysis of $\text{B}(\text{C}_6\text{F}_5)_3$ followed by self-condensation of $(\text{C}_6\text{F}_5)_2\text{BOH}$, leading to $[(\text{C}_6\text{F}_5)_2\text{B}]_2\text{O}$.

It seems clear now that, in previous reports,^{12,13} the failure to observe a reaction between $\text{B}(\text{C}_6\text{F}_5)_3$ and highly dehydroxylated silica was due to the absence of this trace H_2O . Hydrolysis of $\text{B}(\text{C}_6\text{F}_5)_3$, affording $(\text{C}_6\text{F}_5)_2\text{BOH}$, did not occur to an appreciable extent in those experiments because of the prior thermal treatment of the silica, which precluded further silanol condensation.

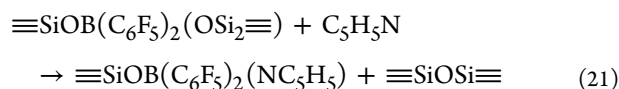
Boron Coordination Number in $\equiv\text{SiOB}(\text{C}_6\text{F}_5)_2$. The value of $\Delta\delta_{m,p}$ in the ^{19}F chemical shifts of (pentafluorophenyl)boranes is a sensitive probe of the boron coordination number.³² Neutral, tetra-coordinate adducts of $\text{B}(\text{C}_6\text{F}_5)_3$ have much smaller $\Delta\delta_{m,p}$ values (e.g., 7.2 ppm for $(\text{C}_6\text{F}_5)_3\text{B}\cdot\text{NC}_5\text{H}_5$, compared to 20.1 ppm for $\text{B}(\text{C}_6\text{F}_5)_3$).^{12,39} When an electron-withdrawing C_6F_5 substituent is replaced by an electron-donating group, such as OH or OR, the $\Delta\delta_{m,p}$ values are slightly smaller for the same boron coordination number. For example, $\Delta\delta_{m,p}$ values for the tri-coordinate boron in $\text{XOB}(\text{C}_6\text{F}_5)_2$ (X = H, CH_3 , or C_6F_5) range from 12 to 15 ppm.⁴⁰ The ^{19}F NMR signals of *endo*-3,7,14-tris{[bis(pentafluorophenyl)boryl]oxy}-1,3,5,7,9,11,14-heptacyclopentyltricyclo[7.3.3.1]heptasiloxane ($\text{T}_7(\text{OB}(\text{C}_6\text{F}_5)_2)_3$), prepared by the reaction of $\text{XB}(\text{C}_6\text{F}_5)_2$ (X = H or Cl) with the corresponding silsesquioxane trisilanol, appear at -131.8 , -148.5 , and -161.3 ppm, corresponding to $\Delta\delta_{m,p} = 13$ ppm. For the silica-supported borane, $\Delta\delta_{m,p}$ is 14 ppm, consistent with tri-coordination at boron.

The boron environment in $\equiv\text{SiOB}(\text{C}_6\text{F}_5)_2$ is also reflected in the solid-state ^{11}B MAS NMR spectrum ($I = 3/2$). The boron coordination number affects the signal line shape, since tri-coordinate boron compounds have high quadrupolar coupling constants (e.g., 2.8–3.3 MHz for boronic acids),⁴¹ resulting in second-order quadrupole broadening even under fast MAS conditions.²⁹ In contrast, tetra-coordinate boron compounds typically give sharp signals due to their relatively low quadrupolar coupling constants (e.g., 0.5–0.8 MHz for the BO_4^{5-} units in borosilicate glasses).⁴² A weak, broad signal with a complex line shape extending from 10 to 40 ppm was found for $\equiv\text{SiOB}(\text{C}_6\text{F}_5)_2$. This line shape is consistent with tri-coordinate boron in solid materials.^{41–43} Upon coordination of $\text{C}_5\text{H}_5\text{N}$, a much sharper, symmetrical peak was observed. At -1.0 ppm, its chemical shift compares well with -3.7 ppm reported for $(\text{C}_6\text{F}_5)_3\text{B}\cdot\text{NC}_5\text{H}_5$ in C_6D_6 .¹³ In the TPD experiment, the appearance of one, symmetrical signal for $\text{C}_5\text{H}_5\text{N}$ desorption indicates that the $\text{C}_5\text{H}_5\text{N}$ adduct is uniform.

We cannot exclude weak coordination of a surface siloxane to some of the $\equiv\text{SiOB}(\text{C}_6\text{F}_5)_2$ sites (eq 20). However, the



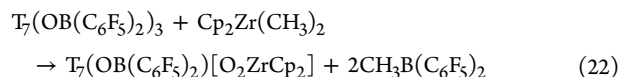
appearance of only one set of three signals for the C_6F_5 ligands in the solid-state ^{19}F MAS NMR spectrum (Figure 5) suggests that $\equiv\text{SiOB}(\text{C}_6\text{F}_5)_2(\text{OSi}\equiv)$ is no more than a minority species. If present, the siloxane should be readily displaced upon $\text{C}_5\text{H}_5\text{N}$ adsorption (eq 21).



Lewis Acidity of $\equiv\text{SiOB}(\text{C}_6\text{F}_5)_2$. The IR spectrum of $\text{C}_5\text{H}_5\text{N}$ adsorbed on oxide surfaces can reveal information about the types (Bronsted/Lewis) and strength of acid sites present.³⁰ $\text{C}_6\text{F}_5\text{N}$ is not strongly adsorbed by silica, consistent with the absence of acidity in unmodified SiO_2 . The IR spectrum of $\equiv\text{SiOB}(\text{C}_6\text{F}_5)_2$ after exposure to $\text{C}_5\text{H}_5\text{N}$ contains a new band at 1632 cm^{-1} , characteristic of $\text{C}_5\text{H}_5\text{N}$ bound to Lewis acid sites.³⁰ Its position indicates that the Lewis acid sites on the borane-modified silica are stronger than those present on the surfaces of either $\gamma\text{-Al}_2\text{O}_3$ or $\text{SiO}_2\text{-Al}_2\text{O}_3$. There is no indication of pyridinium ions (1547 cm^{-1}) or $\text{C}_5\text{H}_5\text{N}$ interacting with hydroxyl groups via hydrogen-bonding (1597 and 1446 cm^{-1}), consistent with our assignment of the residual $\nu(\text{OH})$ bands to inaccessible silanols. The changes in the IR spectrum are very similar to those reported for formation of the molecular adduct $\text{B}(\text{C}_6\text{F}_5)_3\cdot\text{NC}_5\text{H}_5$.¹³

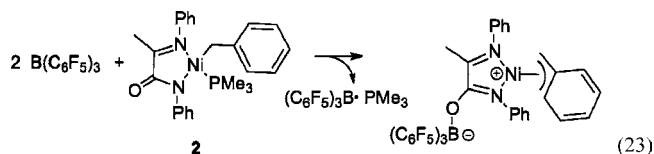
C_2H_4 Polymerization Using $\text{B}(\text{C}_6\text{F}_5)_3$ -Modified Silica as a Cocatalyst. We investigated the ability of silica-supported $\text{B}(\text{C}_6\text{F}_5)_3$ to activate two different single-site olefin polymerization catalysts. Attempts to activate $\text{Cp}_2\text{Zr}(\text{CH}_3)_2$ by its reaction with $\text{B}(\text{C}_6\text{F}_5)_3$ -modified silica failed to yield any polymer. In the supernatant recovered from solution-phase grafting, $(\text{CH}_3)_2\text{B}(\text{C}_6\text{F}_5)$ and $\text{Cp}_2\text{Zr}(\text{CH}_3)(\text{C}_6\text{F}_5)$ were observed, as well as ^{19}F signals tentatively assigned to the unstable ion-pair $[\text{Cp}_2\text{ZrCH}_3^+][(\text{CH}_3)_2\text{B}(\text{C}_6\text{F}_5)_2^-]$. This finding is

consistent with a report that $\text{Cp}_2\text{Zr}(\text{CH}_3)_2$ displaces the borane anchored to a silsesquioxane (eq 22).^{17b} $\text{CH}_3\text{B}(\text{C}_6\text{F}_5)_2$

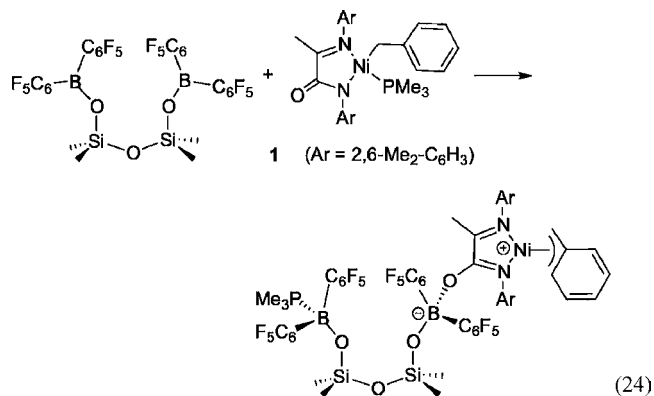


reacted further with $\text{Cp}_2\text{Zr}(\text{CH}_3)_2$ to form $[\text{Cp}_2\text{ZrCH}_3^+][(\text{CH}_3)_2\text{B}(\text{C}_6\text{F}_5)_2^-]$, which decomposed to $\text{Cp}_2\text{Zr}(\text{CH}_3)(\text{C}_6\text{F}_5)$ and $(\text{CH}_3)_2\text{B}(\text{C}_6\text{F}_5)$ over a period of 1 h at room temperature.^{12,17b,31} Thus, a mixture of $\text{T}_7(\text{OB}(\text{C}_6\text{F}_5)_2)_3$ and $\text{Cp}_2\text{Zr}(\text{CH}_3)_2$ was found to be capable of polymerizing C_2H_4 only when prepared *in situ*, and the active site was not associated with the silsesquioxane.

Ethylene polymerization was achieved by combining the late transition metal catalyst **1** with the supported borane as cocatalyst. Complex **1** is inactive in solution at $40\text{ }^\circ\text{C}$, even in the presence of $\text{Ni}(\text{COD})_2$ as a phosphine scavenger. Furthermore, homogeneous catalyst–co-catalyst combinations produce only low-molecular-weight ethylene oligomers.^{18b} However, when **1** was combined with the $\text{B}(\text{C}_6\text{F}_5)_3$ -modified silica, polyethylene was readily obtained at $40\text{ }^\circ\text{C}$. The closely related complex [*N*-phenyl-2-(phenylimino)propanamidato- κ^2 -*N,N*](η^1 -benzyl)-(trimethylphosphine)nickel(II) (**2**) was reported to react with 2 equiv of $\text{B}(\text{C}_6\text{F}_5)_3$ according to eq 23,^{18a} although again only oligomers were generated when the zwitterion was exposed to ethylene.



In the ^{11}B MAS NMR spectrum of **1** adsorbed on $\equiv\text{SiOB}(\text{C}_6\text{F}_5)_2$, the chemical shifts of both peaks are characteristic of tetra-coordinate boron, and their similar intensities suggest that **1** reacts with 2 equiv of $\equiv\text{SiOB}(\text{C}_6\text{F}_5)_2$ in a manner analogous to the homogeneous reaction. Equivalently, the $\equiv\text{SiOB}(\text{C}_6\text{F}_5)_2$ site of the vicinal pair extracts a PMe_3 ligand, and then a second $\equiv\text{SiOB}(\text{C}_6\text{F}_5)_2$ site immobilizes and activates the catalyst by binding to the carbonyl group of the supporting ligand (eq 24).



The ethylene polymerization activity of supported **1** is comparable to that of its homogeneous, $\text{B}(\text{C}_6\text{F}_5)_3$ -activated analogues,^{18a} and the low polydispersity index (2.2) of the resulting polyethylene confirms the single-site nature of the supported catalyst. The much higher molecular weight of the polymer ($M_w = 185\,000$) compared to that of the oligomers

made using the $B(C_6F_5)_3$ -activated catalyst (in the absence of bulky pseudoaxial substituents) is therefore attributed to a support effect. We reported a similar finding with this family of Ni catalysts supported on and activated by strongly Lewis acidic montmorillonite clay.⁴⁴ In both cases, the large steric requirement of the oxide surface presumably restricts the mobility of the active sites and blocks one pseudoaxial position of the catalyst,^{19a} thereby slowing chain transfer to the monomer.

CONCLUSIONS

The reaction of $B(C_6F_5)_3$ with silica, both at ambient temperature and at 100 °C, transforms surface hydroxyl groups into $(\equiv SiO)_n(B(C_6F_5)_{3-n})$ sites and liberates C_6F_5H . However, the grafting reaction is not a simple protonolysis; it requires water as a catalyst. On silicas with high hydroxyl densities, $B(C_6F_5)_3$ appears to promote the condensation of nonvicinal hydroxyl pairs to give relatively unstrained siloxane rings. This does not occur for dehydrated silicas with low surface hydroxyl densities, implying that the formation of $(C_6F_5)_3B\cdot OH_2$ is not capable of inducing condensation to form highly strained siloxane rings. Extrinsic water can also serve as the grafting catalyst. When $B(C_6F_5)_3$ is present in excess, the added H_2O is consumed by eventual formation of $[(C_6F_5)_2B]_2O$. Solid-state ^{19}F and ^{11}B MAS NMR spectroscopy reveal that the grafted borane, formulated as $\equiv SiOB(C_6F_5)_2$ on silica partially dehydroxylated at 500 °C, is tri-coordinate. These sites are uniform and strongly Lewis acidic, based on their reaction with C_5H_5N . Although their reaction with $Cp_2Zr(CH_3)_2$ is complicated, the $B(C_6F_5)_3$ -modified silica is capable of acting cleanly as a cocatalyst for Ni(II) complexes in C_2H_4 polymerization.

EXPERIMENTAL SECTION

Materials and General Methods. Aerosil-380, a fumed silica from Evonik-Degussa, has a BET surface area of $380 \pm 30 \text{ m}^2/\text{g}$ (calculated using $a(N_2) = 0.162 \text{ nm}^2$),⁴⁵ an average primary particle size of 7 nm, and no appreciable microporosity. It was thermally pretreated under vacuum (10^{-4} Torr) at either 200 or 500 °C for 4 h. The resulting silicas are denoted A380-200 and A380-500, respectively. A380-200 contains 1.43 mmol/g of accessible OH groups (denoted $\equiv SiOH$), while A380-500 contains 0.89 mmol/g of $\equiv SiOH$, as measured by $VOCl_3$ chemisorption.²⁷ The absence of physisorbed water on both A380-200 and A380-500 was confirmed by the complete disappearance of the bending mode $\delta(HOH)$ at ca. 1635 cm^{-1} in the IR spectrum.

$B(C_6F_5)_3$ and Cp_2ZrMe_2 (Aldrich) were used as received. The purity of $B(C_6F_5)_3$ was verified by solution-state ^{19}F NMR; only the expected three signals²² were observed. [*N*-(2,6-Dimethylphenyl)-2-(2,6-dimethylphenylimino)propanamidato- κ^2 -*N,N'*](η^1 - CH_2Ph)-(PMe₃)nickel(II) (**1**) was prepared according to a reported procedure.^{18b} Both toluene-*d*₀ and toluene-*d*₈ (Aldrich) were dried over Na/benzophenone, while C_5H_5N (Aldrich) was dried over CaH_2 . All experiments were carried out under rigorously O_2 - and moisture-free conditions using Schlenk-line (10^{-2} Torr), high-vacuum line (10^{-4} Torr), and inert-atmosphere glovebox techniques. A boron standard solution ($H_3BO_3(aq)$, 1000 ppm, Aldrich) was diluted to the desired concentration with deionized water for use in elemental analysis.

Solution-state 1H and ^{19}F NMR spectra were recorded on a Bruker DMX 500 MHz spectrometer, equipped with a 5 mm BBFO 1H - 19F probe, and referenced to $Si(CH_3)_4$ (0 ppm) and $CFCl_3$ (0 ppm), respectively. Solid-state 1H MAS NMR spectra were recorded on a Bruker IP50 500 MHz WB spectrometer. Solid-state ^{11}B and ^{19}F MAS NMR spectra were recorded on either a Bruker DSX 300 MHz WB or a Bruker IP50 500 MHz WB spectrometer. Both solid-state NMR spectrometers are equipped with 4 mm MAS probes. Chemical shifts

are given relative to the following references: 1H , TMS at 0.25 ppm; ^{11}B , $BF_3\cdot OEt_2$ at 0 ppm; ^{19}F , Teflon at -122 ppm.

IR spectra were recorded under Ar in transmission mode on a Bruker ALPHA spectrometer. For background and sample spectra, 32 scans were recorded at a resolution of 4 cm^{-1} . Self-supporting pellets of silica and $B(C_6F_5)_3$ -modified silica were made by pressing 5–10 mg of sample into disks of diameter 7 mm using a hand press. Boron content was determined at 182.641 nm, using an inductively coupled plasma atomic emission spectrometer (Thermo iCAP 6300). Zr and C analyses were performed by Columbia Analytical Services (Tucson, AZ).

Computational Modeling. Geometry optimizations and energy calculations for model compounds were performed with GAUSSIAN03,⁴⁶ using the BP86 exchange correlation. The def2-TZVPP basis set²⁰ was used for all atoms. Stationary points were characterized by the calculation of vibrational frequencies, and all geometries were found to be minimum energy structures ($N_{\text{imaginary}} = 0$).

Solid-Solid Reaction of $B(C_6F_5)_3$ with A380-200 Silica. Thermally pretreated silica (1.000 \pm 0.002 g, containing 1.43 mmol of accessible $\equiv SiOH$) and $B(C_6F_5)_3$ (323.3 mg, 0.600 mmol) were loaded into a Schlenk tube under argon. Dry toluene (15 mL) was vapor-transferred into the reactor, and the slurry was stirred under Ar for 4 h at room temperature. The solvent was removed under a vacuum and the solid stored under Ar at room temperature. To identify soluble intermediates and products, ca. 50 mg portions of the solid were removed and washed with toluene-*d*₈. Solution-state 1H and ^{19}F NMR spectra of the recovered toluene-*d*₈ solutions were recorded.

NMR Tube Reactions of $B(C_6F_5)_3$ with Silica. $B(C_6F_5)_3$ (6.2 mg, 0.012 mmol) was combined with either A380-200 (20.0 mg, containing 0.029 mmol of accessible $\equiv SiOH$) or A380-500 (26.6 mg, containing 0.024 mmol of accessible $\equiv SiOH$) under Ar in the presence of toluene-*d*₈ (0.6 mL) in a solution-state NMR tube (4 mm i.d.) equipped with an air-free valve (Wilmad-Labglass). After three freeze-pump-thaw cycles, the NMR tube was heated to 100 °C in an oil bath. Solution-state 1H and ^{19}F NMR spectra were recorded at room temperature after 1 h, 2.5 h, and 3 d.

Grafting Catalyzed by the Addition of H_2O . A380-500 (0.500 g, containing 0.445 mmol of accessible $\equiv SiOH$) and $B(C_6F_5)_3$ (1124 mg, 2.09 mmol) were combined in a Schlenk tube under Ar, to which was added a mixture of toluene (30 mL) and deionized water (0.75 μL , 0.042 mmol). After three freeze-pump-thaw cycles, the slurry was stirred at 100 °C for 3 d. The solid product was collected on a medium glass frit and then washed with dry toluene ($3 \times 10 \text{ mL}$). The powder was transferred to a glass reactor and dried at 100 °C under vacuum (10^{-4} Torr) for 2.5 h to give a solid containing 0.72 wt % B. It was stored under Ar until use. $B(C_6F_5)_3$ -modified silicas used as cocatalysts (see below) were prepared in the same manner.

Reaction of $(C_6F_5)_2BOH$ with A380-500. $(C_6F_5)_2BOH$ was prepared in a NMR tube by the reaction of $B(C_6F_5)_3$ (11.9 mg, 0.022 mmol) with 1 equiv of H_2O (0.4 μL , 0.022 mmol) in toluene-*d*₈ (0.6 mL) at 70 °C for 30 h.¹² The expected white precipitate of $[(C_6F_5)_2BOH]_3$ was observed.^{17b} A380-500 (43.9 mg, containing 0.0357 mmol of accessible $\equiv SiOH$) was added, and the NMR tube was subjected to three freeze-pump-thaw cycles, followed by heating to 100 °C for 1 h, 2.5 h, or 3 d.

Temperature-Programmed Desorption (TPD). C_5H_5N (60.3 mg, 0.76 mmol) was vapor-transferred onto $B(C_6F_5)_3$ -modified A380-500 (160 mg, 0.11 of mmol B) at room temperature. After 20 min, physisorbed C_5H_5N was removed under a vacuum at the same temperature. A portion of this solid (ca. 40 mg) was loaded into a quartz micro-reactor (Hiden CATLAB, $18.50 \times 0.48 \text{ cm}$ i.d.) to give a bed of length ca. 1.5 cm, held in place with plugs of quartz wool. The temperature was monitored by a K-type thermocouple touching the sample bed. An inlet gas flow rate (Ar) of 50 mL min^{-1} was maintained using a mass flow controller. C_5H_5N desorption was monitored online with an online quadrupole mass spectrometer (HR-20, Hiden Analytical) while the temperature was ramped at $5 \text{ }^\circ\text{C min}^{-1}$. A secondary electron multiplier (SEM) detector was used to monitor the MS signal at $m/z = 79$ ($C_5H_5N^+$). The electron energy and emission current were set to 70.0 eV and 250 μA , respectively.

Reactions of B(C₆F₅)₃-Modified Silica with Cp₂ZrMe₂ and Attempted C₂H₄ Polymerization. B(C₆F₅)₃-modified A380-500 (30 mg, 0.020 mmol B) was loaded into a glass reactor equipped with a break-seal containing Cp₂ZrMe₂ (7.3 mg, 0.028 mmol). Cp₂ZrMe₂ was sublimed for 2 d under reduced pressure (10⁻⁴ Torr) onto the B(C₆F₅)₃-modified silica with the aid of a liquid N₂ bath. The solid mixture was allowed to warm to room temperature, and the reaction was allowed to proceed for 1 d. Unreacted Cp₂ZrMe₂ was then desorbed to the break-seal side arm at the same temperature for a further 2 d, at which time it was flame-sealed and removed. The resulting product was a white solid. C₂H₄ (111 Torr, Praxair, 99.999%) was transferred into the reactor at room temperature, and C₂H₄ uptake was monitored using a capacitance manometer (MKS, 0.1–1000 Torr).

To investigate the formation of soluble products, the reaction of B(C₆F₅)₃-modified A380-500 (11.5 mg, 0.0077 mmol B) with Cp₂ZrMe₂ (2.8 mg, 0.011 mmol) dissolved in toluene-d₈ (0.8 mL) was carried out in a NMR tube at room temperature. Solution-state ¹H and ¹⁹F NMR spectra were recorded 40 min after the mixture was prepared.

Reaction of B(C₆F₅)₃-Modified Silica with [N-(2,6-Dimethylphenyl)-2-(2,6-dimethylphenylimino)propanamido-κ⁻²-N,N](η¹-CH₂Ph)(PMe₃)nickel(II) (1), and C₂H₄ Polymerization. Under N₂, **1** (3.5 mg, 0.0067 mmol) was dissolved in toluene (30 mL), and the resulting solution was transferred to the glass insert of a 100 mL Parr reactor containing B(C₆F₅)₃-modified A380-500 (50 mg, 0.033 mmol B). The mixture was heated to 40 °C with continuous stirring, and then C₂H₄ (5.2 × 10³ Torr) was added on demand for 30 min. The pressure was released, and the product was precipitated with acetone, filtered, washed with acetone, and air-dried.

A similar mixture of **1** and B(C₆F₅)₃-modified A380-500 was stirred in toluene (10 mL) for 3 h. After solvent removal under reduced pressure for 1 h, the solid-state ¹¹B NMR spectrum of the solid was recorded at 160.419 MHz.

■ ASSOCIATED CONTENT

■ Supporting Information

Optimized energies and Cartesian coordinates for all calculated structures, C₅H₅N-TPD profile, additional NMR spectra, and complete ref 46. This material is available free of charge via the Internet at <http://pubs.acs.org>.

■ AUTHOR INFORMATION

Corresponding Author

sscott@engineering.ucsb.edu

■ ACKNOWLEDGMENTS

We thank Drs. Jenny McCahill and Gregory Welch for helpful discussions. This work was supported by the National Science Foundation under Grant No. CBET08-54425. Portions of this work were performed using the Central Facilities of the Materials Research Laboratory, supported by the MRSEC Program of the NSF under Award No. DMR 1121053 and a member of the NSF-funded Materials Research Facilities Network (www.mrfn.org).

■ REFERENCES

- (1) Chen, E. Y. X.; Marks, T. J. *Chem. Rev.* **2000**, *100*, 1391–1434.
- (2) (a) Yang, X. M.; Stern, C. L.; Marks, T. J. *J. Am. Chem. Soc.* **1991**, *113*, 3623–3625. (b) Yang, X. M.; Stern, C. L.; Marks, T. J. *J. Am. Chem. Soc.* **1994**, *116*, 10015–10031.
- (3) Boardman, B. M.; Bazan, G. C. *Acc. Chem. Res.* **2009**, *42*, 1597–1606.
- (4) Clark, J. H. *Acc. Chem. Res.* **2002**, *35*, 791–797.
- (5) Sreekanth, P.; Kim, S.-W.; Hyeon, T.; Kim, B. M. *Adv. Synth. Catal.* **2003**, *345*, 936–938.
- (6) Hlatky, G. G. *Chem. Rev.* **2000**, *100*, 1347–1376.

(7) Fink, G.; Steinmetz, B.; Zechlin, J.; Przybyla, C.; Tesche, B. *Chem. Rev.* **2000**, *100*, 1377–1390.

(8) Iler, R. K. *The Chemistry of Silica: Solubility, Polymerization, Colloid and Surface Properties and Biochemistry of Silica*; Wiley: New York, 1979.

(9) Zurek, E.; Ziegler, T. *Prog. Polym. Sci.* **2004**, *29*, 107–148.

(10) (a) Walzer, J. F., Jr. U.S. Patent 5,643,847, 1997. (b) Holtcamp, M. W.; Lue, C.-T. U.S. Patent 6,476,166, 2002. (c) Holtcamp, M. W.; Cano, D. A. U.S. Patent 6,703,338, 2004.

(11) Charoenchaidet, S.; Chavadej, S.; Gulari, E. *J. Mol. Catal. A: Chem.* **2002**, *185*, 167–177.

(12) Tian, J.; Wang, S.; Feng, Y.; Li, J.; Collins, S. *J. Mol. Catal. A: Chem.* **1999**, *144*, 137–150.

(13) Millot, N.; Santini, C. C.; Lefebvre, F.; Basset, J.-M. *C. R. Chim.* **2004**, *7*, 725–736.

(14) (a) McKinley, S. G.; Vecchi, P. A.; Ellern, A.; Angelici, R. J. *Dalton Trans.* **2004**, 788–793. (b) Wiench, J. W.; Michon, C.; Ellern, A.; Hazendonk, P.; Iuga, A.; Angelici, R. J.; Pruski, M. *J. Am. Chem. Soc.* **2009**, *131*, 11801–11810.

(15) (a) Ward, D. G.; Carnahan, E. M. U.S. Patent 5,939,347, 1996. (b) Hikuma, S.; Kibino, N.; Hori, A.; Myake, S.; Inasawa, S. Japanese Patent 08 113604, 1996. (c) Kristen, M. O.; Lynch, J.; Lux, M.; Lange, A.; Karer, R. *Proceedings of Metallocenes Europe, '97 Conference*, Düsseldorf, 1997. (d) Carney, M. J.; Shih, K. Y. *Proceedings of Metallocenes Europe, '98 Conference*, Düsseldorf, 1998. (e) Walzer, J. F. *Abstr. Papers Am. Chem. Soc.* **1998**, *215*, U714 (051-Inor, Apr 2). (f) Bochmann, M.; Pindado, G. J.; Lancaster, S. J. *J. Mol. Catal. A: Chem.* **1999**, *146*, 179–190. (g) Kristen, M. O. *Top. Catal.* **1999**, *7*, 89–95. (h) Millot, N.; Cox, A.; Santini, C. C.; Molard, Y.; Basset, J. M. *Chem.—Eur. J.* **2002**, *8*, 1438–1442. (i) Charoenchaidet, S.; Chavadej, S.; Gulari, E. *J. Polym. Sci., Polym. Chem.* **2002**, *40*, 3240–3248. (j) Panchenko, V. N.; Danilova, I. G.; Zakharov, V. A.; Paukshtis, E. A. *J. Mol. Catal. A: Chem.* **2005**, *225*, 271–277.

(16) (a) Millot, N.; Santini, C. C.; Baudouin, A.; Basset, J.-M. *Chem. Commun.* **2003**, 2034–2035. (b) Millot, N.; Soignier, S.; Santini, C. C.; Baudouin, A.; Basset, J.-M. *J. Am. Chem. Soc.* **2006**, *128*, 9361–9370.

(17) (a) Duchateau, R.; van Santen, R. A.; Yap, G. P. A. *Organometallics* **2000**, *19*, 809–816. (b) Metcalfe, R. A.; Kreller, D. I.; Tian, J.; Kim, H.; Taylor, N. J.; Corrigan, J. F.; Collins, S. *Organometallics* **2002**, *21*, 1719–1726.

(18) (a) Lee, B. Y.; Bazan, G. C.; Vela, J.; Komon, Z. J. A.; Bu, X. H. *J. Am. Chem. Soc.* **2001**, *123*, 5352–5353. (b) Rojas, R. S.; Wasilke, J.-C.; Wu, G.; Ziller, J. W.; Bazan, G. C. *Organometallics* **2005**, *24*, 5644–5653.

(19) (a) Ittel, S. D.; Johnson, L. K.; Brookhart, M. *Chem. Rev.* **2000**, *100*, 1169–1203. (b) Nakamura, A.; Ito, S.; Nozaki, K. *Chem. Rev.* **2009**, *109*, 5215–5244.

(20) Timoshkin, A. Y.; Frenking, G. *Organometallics* **2008**, *27*, 371–380.

(21) Liu, C. H. C.; Maciel, G. E. *J. Am. Chem. Soc.* **1996**, *118*, 5103–5119.

(22) Beringhelli, T.; D'Alfonso, G.; Donghi, D.; Maggioni, D.; Mercandelli, P.; Sironi, A. *Organometallics* **2004**, *23*, 5493–5502.

(23) Bruce, M. I. *J. Chem. Soc. A* **1968**, 1459–1464.

(24) (a) Doremus, R. H. *J. Mater. Res.* **1995**, *10*, 2379–2389. (b) Van Ginhoven, R. M.; Jonsson, H.; Park, B.; Corrales, L. R. *J. Phys. Chem. B* **2005**, *109*, 10936–10945.

(25) Taha, Z. A.; Deguns, E. W.; Chattopadhyay, S.; Scott, S. L. *Organometallics* **2006**, *25*, 1891–1899.

(26) Bunker, B. C.; Haaland, D. M.; Michalske, T. A.; Smith, W. L. *Surf. Sci.* **1989**, *222*, 95–118.

(27) Rice, G. L.; Scott, S. L. *Langmuir* **1997**, *13*, 1545–1551.

(28) (a) Morrow, B. A.; Devi, A. *J. Chem. Soc., Faraday Trans.* **1972**, *68*, 403–422. (b) Possemiers, K.; VanDerVoort, P.; Vansant, E. F. *J. Chem. Soc., Faraday Trans.* **1996**, *92*, 679–684.

(29) Engelhardt, G.; Michel, D. *High-Resolution Solid-State NMR of Silicates and Zeolites*; Wiley: Chichester, UK, 1987.

(30) Busca, G. *Catal. Today* **1998**, *41*, 191–206.

- (31) Kohler, K.; Piers, W. E.; Jarvis, A. P.; Xin, S.; Feng, Y.; Bravakis, A. M.; Collins, S.; Clegg, W.; Yap, G. P. A.; Marder, T. B. *Organometallics* **1998**, *17*, 3557–3566.
- (32) Beringhelli, T.; Donghi, D.; Maggioni, D.; D'Alfonso, G. *Coord. Chem. Rev.* **2008**, *252*, 2292–2313.
- (33) Welch, G. C.; Holtrichter-Roessmann, T.; Stephan, D. W. *Inorg. Chem.* **2008**, *47*, 1904–1906.
- (34) Brinker, C. J.; Kirkpatrick, R. J.; Tallant, D. R.; Bunker, B. C.; Montez, B. J. *Non-Cryst. Solids* **1988**, *99*, 418–428.
- (35) Bergquist, C.; Bridgewater, B. M.; Harlan, C. J.; Norton, J. R.; Friesner, R. A.; Parkin, G. J. *Am. Chem. Soc.* **2000**, *122*, 10581–10590.
- (36) (a) Gouzyr, A. I.; Wessel, H.; Barnes, C. E.; Roesky, H. W.; Teichert, M.; Uson, I. *Inorg. Chem.* **1997**, *36*, 3392–3393. (b) Guzyr, O. I.; Prust, J.; Roesky, H. W.; Lehmann, C.; Teichert, M.; Cimpoesu, F. *Organometallics* **2000**, *19*, 1549–1555.
- (37) Winkhofer, N.; Roesky, H. W.; Noltemeyer, M.; Robinson, W. T. *Angew. Chem., Int. Ed.* **1992**, *31*, 599–601.
- (38) Fleischman, S. D. F. S. D.; Scott, S. L. *J. Am. Chem. Soc.* **2011**, *133*, 4847–4855.
- (39) Blackwell, J. M.; Piers, W. E.; Parvez, M. *Org. Lett.* **2000**, *2*, 695–698.
- (40) Britovsek, G. J. P.; Ugolotti, J.; White, A. J. P. *Organometallics* **2005**, *24*, 1685–1691.
- (41) Weiss, J. W. E.; Bryce, D. L. *J. Phys. Chem. A* **2010**, *114*, 5119–5131.
- (42) Soraru, G. D.; Dallabona, N.; Gervais, C.; Babonneau, F. *Chem. Mater.* **1999**, *11*, 910–919.
- (43) (a) Scholle, K.; Veeman, W. S. *Zeolites* **1985**, *5*, 118–122. (b) Hwang, S. J.; Fernandez, C.; Amoureux, J. P.; Cho, J.; Martin, S. W.; Pruski, M. *Solid State Nucl. Magn. Reson.* **1997**, *8*, 109–121. (c) Bray, P. J. *Inorg. Chim. Acta* **1999**, *289*, 158–173. (d) Bryce, D. L.; Wasylshen, R. E.; Gee, M. J. *Phys. Chem. A* **2001**, *105*, 3633–3640. (e) Hwang, S. J.; Chen, C. Y.; Zones, S. I. *J. Phys. Chem. B* **2004**, *108*, 18535–18546.
- (44) Scott, S. L.; Peoples, B. C.; Yung, C.; Rojas, R. S.; Khanna, V.; Sano, H.; Suzuki, T.; Shimizu, F. *Chem. Commun.* **2008**, 4186–4188.
- (45) Jelinek, L.; Kovats, E. S. *Langmuir* **1994**, *10*, 4225–4231.
- (46) Frisch, M. J.; et al. *Gaussian 03*, Revision C.02; Gaussian, Inc.: Wallingford, CT, 2004.